

## Search for the Blazhko effect in field RR Lyrae stars using LINEAR and ZTF light curves

2 EMA DONEV<sup>1</sup> AND ŽELJKO IVEZIĆ<sup>2</sup>

3 <sup>1</sup>XV. Gymnasium (MIOC), Jordanovac 8, 10000, Zagreb, Croatia

4 <sup>2</sup>Department of Astronomy and the DiRAC Institute, University of Washington, 3910 15th Avenue NE, Seattle, WA 98195, USA

### 5 ABSTRACT

6 We analyzed the incidence and properties of RR Lyrae stars that show evidence for amplitude and  
7 phase modulation (the so-called Blazhko Effect) in a sample of  $\sim$ 3,000 stars with LINEAR and ZTF  
8 light curve data collected during the periods of 2002–2008 and 2018–2023, respectively. A preliminary  
9 subsample of about  $\sim$ 500 stars was algorithmically pre-selected using various data quality and light  
10 curve statistics, and then 228 stars were confirmed visually as displaying the Blazhko effect. This  
11 sample increases the number of field RR Lyrae stars displaying the Blazhko effect by more than 50%  
12 and places a lower limit of  $(11.4 \pm 0.8)\%$  for their incidence rate. We find that ab type RR Lyrae  
13 that show the Blazhko effect have about 5% (0.030 day) shorter periods than starting sample, a  $7.1\sigma$   
14 statistically significant difference. We find no significant differences in their light curve amplitudes and  
15 apparent magnitude (essentially, signal-to-noise ratio) distributions. No period or other differences are  
16 found for c type RR Lyrae. We find convincing examples of stars where the Blazhko effect can appear  
17 and disappear on time scales of several years. With time-resolved photometry expected from LSST, a  
18 similar analysis will be performed for even larger samples of fields RR Lyrae stars in the southern sky  
19 and we anticipate a higher fraction of discovered Blazhko stars due to better sampling and superior  
20 photometric quality.

21 *Keywords:* Variable stars — RR Lyrae variable stars — Blazhko effect

### 22 1. INTRODUCTION

23 RR Lyrae stars are pulsating variable stars with peri-  
24 ods in the range of 3–30 hours and large amplitudes that  
25 increase towards blue optical bands (e.g., in the SDSS *g*  
26 band from 0.2 mag to 1.5 mag; Sesar et al. 2010). For  
27 comprehensive reviews of RR Lyrae stars, we refer the  
28 reader to Smith (1995) and Catelan (2009).

29 RR Lyrae stars often exhibit amplitude and phase  
30 modulation, or the so-called Blazhko effect<sup>1</sup> (hereafter,  
31 “Blazhko stars”). For examples of well-sampled observed  
32 light curves showing the Blazhko effect, see, e.g., Ke-  
33 pler data shown in Figures 1 and 2 from Benkő et al.  
34 (2010). The Blazhko effect has been known for a long  
35 time (Blažko 1907), but its detailed observational prop-  
36 erties and theoretical explanation of its causes remain  
37 elusive (Kolenberg 2008; Kovács 2009; Szabó 2014). Var-  
38 ious proposed models for the Blazhko effect, and prin-  
39 cipal reasons why they fail to explain observations, are  
40 summarized in Kovacs (2016).

Corresponding author: Željko Ivezić  
ivezic@uw.edu

<sup>1</sup> The Blazhko effect was discovered by Lidiya Petrovna Tseraskaya and first reported by Sergey Blazhko.

41 A part of the reason for the incomplete observational  
42 description of the Blazhko effect is difficulties in discov-  
43 ering a large number of Blazhko stars due to tempo-  
44 ral baselines that are too short and insufficient number  
45 of observations per object (Kovacs 2016; Hernitschek &  
46 Stassun 2022). With the advent of modern sky sur-  
47 veys, several studies reported large increases in the num-  
48 ber of known Blazhko stars, starting with a sample of  
49 about 700 Blazhko stars discovered by the MACHO sur-  
50 vey towards the LMC (Alcock et al. 2003) and about  
51 500 Blazhko stars discovered by the OGLE-II survey  
52 towards the Galactic bulge (Mizerski 2003). Most re-  
53 cently, about 4,000 Blazhko stars were discovered in the  
54 LMC and SMC (Soszyński et al. 2009, 2010), and an  
55 additional  $\sim$ 3,500 stars were discovered in the Galactic  
56 bulge (Soszyński et al. 2011; Prudil & Skarka 2017), both  
57 by the OGLE-III survey. Nevertheless, discovering the  
58 Blazhko effect in field RR Lyrae stars that are spread  
59 over the entire sky remains a much harder problem: only  
60 about 400 Blazhko stars in total (Skarka 2013) from all  
61 the studies of field RR Lyrae stars have been reported  
62 so far (see also Table 1 in Kovacs 2016).

63 Here, we report the results of a search for the Blazhko  
64 effect in a sample of  $\sim$ 3,000 field RR Lyrae stars with  
65 LINEAR and ZTF light curve data. A preliminary sub-

sample of about  $\sim 500$  stars was selected using various light curve statistics, and then 228 stars were confirmed visually as displaying the Blazhko effect. This new sample doubles the number of field RR Lyrae stars that exhibit the Blazhko effect. In §2 and §3 we describe our datasets and analysis methodology, and in §4 we present our analysis results. Our main results are summarized and discussed in §5.

## 2. DATA DESCRIPTION AND PERIOD ESTIMATION

Analysis of field RR Lyrae stars requires a sensitive time-domain photometric survey over a large sky area. For our starting sample, we used  $\sim 3,000$  field RR Lyrae stars with light curves obtained by the LINEAR asteroid survey. In order to study long-term changes in light curves, we also utilized light curves obtained by the ZTF survey which monitored the sky  $\sim 15$  years after LINEAR. The combination of LINEAR and ZTF provided a unique opportunity to systematically search for the Blazhko effect in a large number of field RR Lyrae stars over a large time span of two decades.

We first describe each dataset in more detail, and then introduce our analysis methods. All our analysis code, written in Python, is available on GitHub<sup>2</sup>.

### 2.1. LINEAR Dataset

The properties of the LINEAR asteroid survey and its photometric re-calibration based on SDSS data are discussed in Sesar et al. (2011). Briefly, the LINEAR survey covered about  $10,000 \text{ deg}^2$  of the northern sky in white light (no filters were used, see Fig. 1 in Sesar et al. 2011), with photometric errors ranging from  $\sim 0.03$  mag at an equivalent SDSS magnitude of  $r = 15$  to  $0.20$  mag at  $r \sim 18$ . Light curves used in this work include, on average, 270 data points collected between December 2002 and September 2008.

A sample of 7,010 periodic variable stars with  $r < 17$  discovered in LINEAR data were robustly classified by Palaversa et al. (2013), including about  $\sim 3,000$  field RR Lyrae stars of both ab and c type, detected to distances of about 30 kpc (Sesar et al. 2013). The sample used in this work contains 2196 ab-type and 745 c-type RR Lyrae, selected using classification labels and the *gi* color index from Palaversa et al. (2013). The LINEAR light curves, augmented with IDs, equatorial coordinates, and other data, were accessed using the astroML Python module<sup>3</sup> (VanderPlas et al. 2012).

### 2.2. ZTF Dataset

<sup>2</sup> [https://github.com/emadonev/var\\_stars](https://github.com/emadonev/var_stars)

<sup>3</sup> For an example of light curves, see [https://www.astroml.org/book\\_figures/chapter10/fig\\_LINEAR\\_LS.html](https://www.astroml.org/book_figures/chapter10/fig_LINEAR_LS.html)

The Zwicky Transient Factory (ZTF) is an optical time-domain survey that uses the Palomar 48-inch Schmidt telescope and a camera with  $47 \text{ deg}^2$  field of view (Bellm et al. 2019). The dataset analyzed here was obtained with SDSS-like *g*, *r*, and *i* band filters. Light curves for objects in common with the LINEAR RR Lyrae sample typically have smaller random photometric errors than LINEAR light curves because ZTF data are deeper (compared to LINEAR, ZTF data have about 2-3 magnitudes fainter  $5\sigma$  depth). ZTF data used in this work were collected between February 2018 and December 2023, on average about 15 years after obtaining LINEAR data. The median number of observations per star for ZTF light curves is  $\sim 500$ .

The ZTF dataset for this project was created by selecting ZTF IDs with matching equatorial coordinates to a corresponding LINEAR ID of an RR Lyrae star. This process used the *ztfquery* function, which searched the coordinates in the ZTF database within 3 arcsec from the LINEAR position. The resulting sample consisted of 2857 RR Lyrae stars with both LINEAR and ZTF data. The fractions of RRab and RRc type RR Lyrae in this sample, 71% RRab and 29% RRc type, are consistent with results from other surveys (e.g., Sesar et al. 2010).

### 2.3. Period Estimation

The first step of our analysis is estimating best-fit periods, separately for LINEAR and ZTF datasets. We used the Lomb-Scargle method (Vanderplas 2015) as implemented in *astropy* (Astropy Collaboration et al. 2018). The period estimation used 3 Fourier components and a two-step process: an initial best-fit frequency was determined using the *autopower* frequency grid option and then the power spectrum was recomputed around the initial frequency using an order of magnitude smaller frequency step. In case of ZTF, we estimated period separately for each available passband and adopted their median value. Once the best-fit period was determined, a best-fit model for the phased light curve was computed using 6 Fourier components. Fig 1 shows an example of a star with LINEAR and ZTF light curves, phased light curves, and their best-fit models.

We found excellent agreement between the best-fit periods estimated separately from LINEAR and ZTF light curves. The median of their ratio is unity within  $2 \times 10^{-6}$  and the robust standard deviation of their ratio is  $2 \times 10^{-5}$ . With a median sample period of 0.56 days, the implied scatter of period difference is about 1.0 sec.

Given on average about 15 years between LINEAR and ZTF data sets, and a typical period of 0.56 days, this time difference corresponds to about 10,000 oscillations. With a fractional period uncertainty of  $2 \times 10^{-5}$ , LINEAR data can predict the phase of ZTF light curve with an uncertainty of 0.2. Therefore, for a robust detection of light curve phase modulation, each data set must be analyzed separately. On the other hand, ampli-

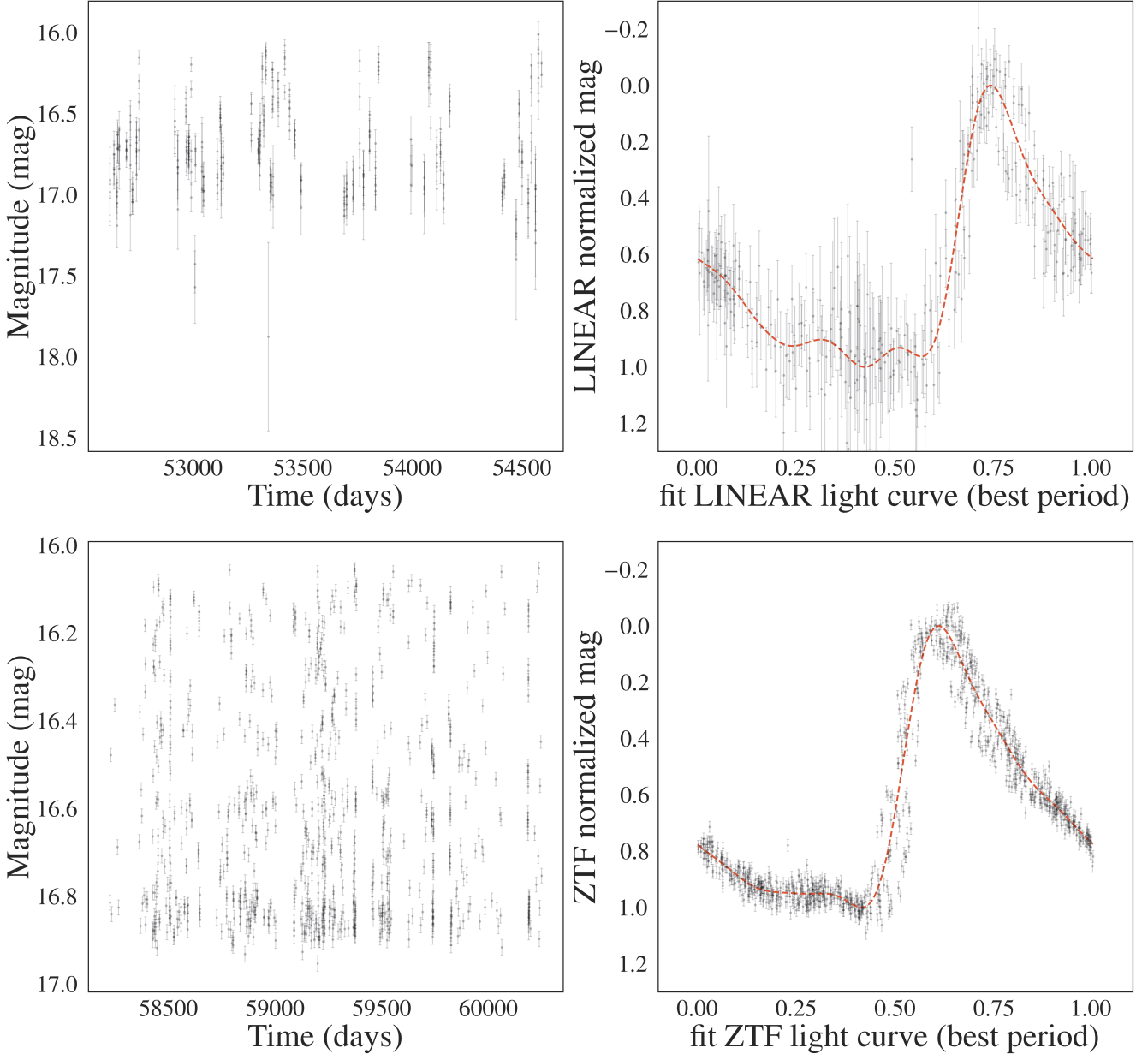


**Figure 1.** An example of a Blazhko star (LINEARid = 136668) with LINEAR (top row) and ZTF (bottom row) light curves (left panels, data points with “error bars”), phased light curves normalized to the 0–1 range (right panels, data points with “error bars”), with their best-fit models shown by dashed lines. The best-fit period is determined for each dataset separately using 3 Fourier terms. The models shown in the right panels are evaluated with 6 Fourier terms.

tude modulation can be detected on time scales as long as 15 years, as discussed in the following section.

### 3. ANALYSIS METHODOLOGY: SEARCHING FOR THE BLAZHKO EFFECT

Given the two sets of light curves from LINEAR and ZTF, we searched for amplitude and phase modulation, either during the 5–6 years of data taking by each survey, or during the average span of 15 years between the two surveys. Starting with a sample of 2857 RR Lyrae stars, we pre-selected a smaller sample that was inspected visually (see below for details). We also re-

quired at least 150 LINEAR data points and 150 ZTF data points (for the selected band from which we calculated the period) in analyzed light curves. We used two pre-selection methods that are sensitive to different types of light curve modulation: direct light curve analysis and periodogram analysis, as follows.

#### 3.1. Direct Light Curve Analysis

Given statistically correct period, amplitude and light curve shape estimates, as well as data being consistent with reported (presumably Gaussian) uncertainty estimates, the  $\chi^2$  per degree of freedom gives a quantitative

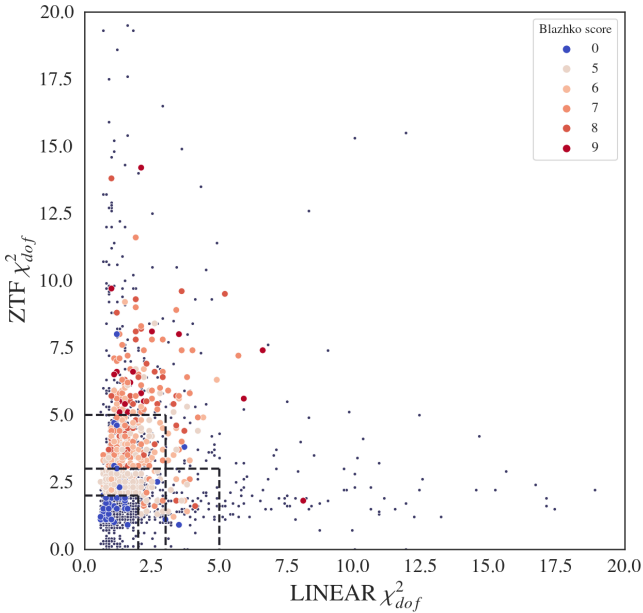


**Figure 2.** A selection diagram constructed with the two sets of robust  $\chi^2_{dof}$  values, for LINEAR and ZTF data sets, where the dark blue dots represent all RR Lyrae stars and the circles represent candidate Blazhko stars (color-coded according to the legend, with B\_score representing the number of points scored from the selection algorithm). The horizontal and vertical dashed lines help visualize selection boundaries for Blazhko candidates (see text).

190 assessment of the "goodness of fit",

$$191 \quad \chi^2_{dof} = \frac{1}{N_{dof}} \sum \frac{(d_i - m_i)^2}{\sigma_i^2}. \quad (1)$$

192 Here,  $d_i$  are measured light curve data values at times  
 193  $t_i$ , and with associated uncertainties  $\sigma_i$ ,  $m_i$  are best-  
 194 fit models at times  $t_i$ , and  $N_{dof}$  is the number of de-  
 195 grees of freedom, essentially the number of data points.  
 196 In the absence of any light curve modulation, the ex-  
 197 pected value of  $\chi^2_{dof}$  is unity, with a standard devia-  
 198 tion of  $\sqrt{2/N_{dof}}$ . If  $\chi^2_{dof} - 1$  is many times larger than  
 199  $\sqrt{2/N_{dof}}$ , it is unlikely that data  $d_i$  were generated by  
 200 the assumed (unchanging) model  $m_i$ . Of course,  $\chi^2_{dof}$   
 201 can also be large due to underestimated measurement  
 202 uncertainties  $\sigma_i$ , or to occasional non-Gaussian measure-  
 203 ment error (the so-called outliers).

204 Therefore, to search for signatures of the Blazhko ef-  
 205 fect, manifested through statistically unlikely large val-  
 206 ues of  $\chi^2_{dof}$ , we computed  $\chi^2_{dof}$  separately for LINEAR  
 207 and ZTF data (see Fig. 2). Using the two sets of  $\chi^2_{dof}$   
 208 values, we algorithmically pre-selected a sample of can-  
 209 didate Blazhko stars for further visual analysis of their  
 210 light curves. The visual analysis is needed to confirm  
 211 the expected Blazhko behavior in observed light curves,  
 212 as well as to identify cases of data problems, such as  
 213 photometric outliers.

214 We used a simple scoring algorithm, optimized  
 215 through trial and error, that utilized the two values of  
 216  $\chi^2_{dof}$ , augmented by period and amplitude differences, as  
 217 follows. A star could score a maximum of 9 points, and  
 218 a minimum of 5 points was required for further visual  
 219 analysis. The  $\chi^2_{dof}$  selection boundaries are illustrated  
 220 in Fig. 2. If either value of  $\chi^2_{dof}$  exceeded 5, or both ex-  
 221 ceeded 3, a star was awarded 5 points and immediately  
 222 selected for further analysis. If these  $\chi^2_{dof}$  criteria were  
 223 not met, a star could still be selected by meeting less  
 224 stringent  $\chi^2_{dof}$  selection if it also had large period or am-  
 225 plitude difference between LINEAR and ZTF datasets.  
 226 Stars with at least one value of  $\chi^2_{dof}$  above 2 would re-  
 227 ceive 3 points and those with at least one  $\chi^2_{dof}$  above  
 228 3 would receive 4 points. A period difference exceeding  
 229  $2 \times 10^{-4}$  day would be awarded 1 point and two points for  
 230 exceeding  $5 \times 10^{-4}$  day. Analogous limits for amplitude  
 231 difference were 0.05 mag and 0.15 mag, respectively.

232 The candidate Blazhko sample pre-selected using this  
 233 method includes 531 stars. For most selected stars, the  
 234  $\chi^2_{dof}$  values were larger for the ZTF data because the  
 235 ZTF photometric uncertainties are smaller than for the  
 236 LINEAR data set. Fig. 3 summarizes the selection cri-  
 237 teria and the resulting numbers of selected stars for each  
 238 criterion and their combinations.

### 3.2. Periodogram Analysis

239 When light curve modulation is due to double-mode  
 240 oscillation with two similar oscillation frequencies (peri-  
 241 ods), it is possible to recognize its signature in the peri-  
 242 odogram computed as part of the Lomb-Scargle analy-  
 243 sis. Depending on various details, such as data sampling  
 244 and the exact values of periods, amplitudes, this method  
 245 may be more efficient than direct light curve analysis  
 246 (Skarka et al. 2020). We also employed this method to  
 247 select additional candidates, as follows.

248 A sum of two *sine* functions with same amplitudes  
 249 and with frequencies  $f_1$  and  $f_2$  can be rewritten using  
 250 trigonometric equalities as

$$252 \quad y(t) = 2 \cos(2\pi \frac{f_1 - f_2}{2} t) \sin(2\pi \frac{f_1 + f_2}{2} t). \quad (2)$$

253 We can define

$$254 \quad f_o = \frac{f_1 + f_2}{2}, \quad (3)$$

255 and

$$256 \quad \Delta f = \left| \frac{f_1 - f_2}{2} \right|, \quad (4)$$

257 with  $\Delta f \ll f_o$  when  $f_1$  and  $f_2$  are similar. The fact  
 258 that  $\Delta f$  is much smaller than  $f_o$  means that the pe-  
 259 riod of the *cos* term is much larger than the period of  
 260 the basic oscillation ( $f_o$ ). In other words, the *cos* term  
 261 acts as a slow amplitude modulation of the basic oscil-  
 262 lation. When the amplitudes of two *sine* functions are  
 263 not equal, the results are more complicated but the basic  
 264 conclusion about amplitude modulation remains. When

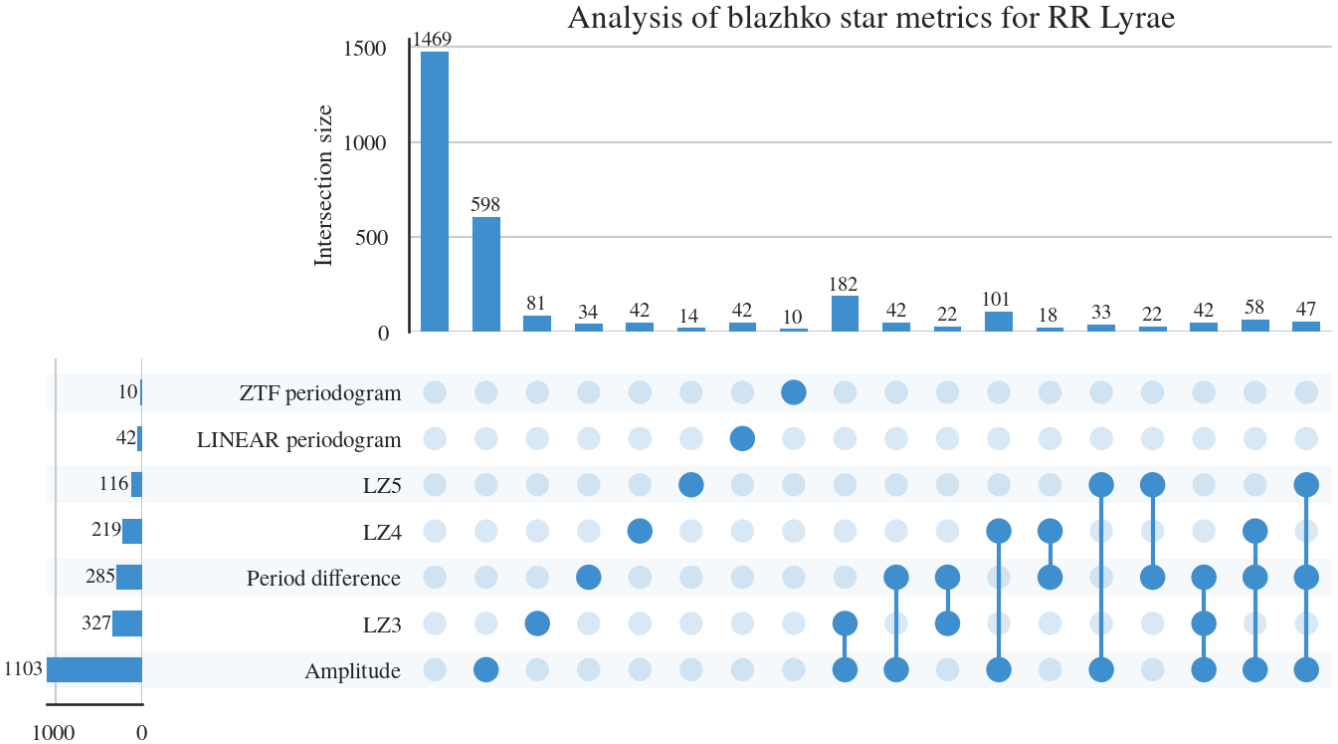


**Figure 3.** The figure shows selection criteria and the resulting numbers of pre-selected Blazhko star candidates for each criterion and their combinations (x in LZx corresponds to the number of scored points in the  $\chi^2_{dof}$  vs.  $\chi^2_{dof}$  diagram (see Fig. 2). The dots represent each case a star can occupy, where every solid dot is a specific criterion that is satisfied. Connections between solid dots represent stars which satisfy multiple criteria. Each dot combination has its own count, represented by the horizontal countplot. The vertical countplot shows the total number of stars that satisfy one criteria (union of all cases). For example, a total of 116 stars passed the LZ5 criterion, with 14 of them satisfying only  $\chi^2$  criterion, 33 also had a significant amplitude change, 22 had a significant period difference, and 47 had both a significant period and amplitude difference along with the satisfied  $\chi^2$  criterion. The sum of all specific cases is 116.

the power spectrum of  $y(t)$  is constructed, it will show 265 3 peaks: the main peak at  $f_o$  and two more peaks at 266 frequencies  $f_o \pm \Delta f$ . We used this fact to construct an 267 algorithm for automated searching for the evidence of 268 amplitude modulation. Fig 4 compares the theoretical 269 periodogram produced by interference beats with our 270 algorithm's periodogram, signifying that local Blazhko 271 peaks are present in real data.

After the strongest peak in the Lomb-Scargle periodogram is found at frequency  $f_o$ , we search for two equally distant local peaks at frequencies  $f_-$  and  $f_+$ , with  $f_- < f_o < f_+$ . The sideband peaks can be highly asymmetric Alcock et al. (2003) and observed periodograms can sometimes be much more complex Szczygieł & Fabrycky (2007). We fold the periodogram through the main peak at  $f_o$ , multiply the two branches and then search for the strongest peaks in the resulting folded periodogram that is statistically more significant than the background noise. The background noise is computed as the scatter of the folded periodogram estimated from the interquartile range. We require a “signal-to-noise” ratio of at least 5, as well as the peak

strength of at least 0.05 for ZTF, while 0.10 for LINEAR data. If such a peak is found, and it doesn't correspond to yearly alias, we select the star as a candidate Blazhko star and compute its Blazhko period as

$$P_{BL} = |f_{-,+} - f_o|^{-1},$$

where  $f_{-,+}$  means the Blazhko sideband frequency with a higher amplitude is chosen.

The observed Blazhko periods range from 3 to 3,000 275 days, and Blazhko amplitudes range from 0.01 mag to 276 about 0.3 mag (Szczygieł & Fabrycky 2007). In this 277 work, we selected a smaller Blazhko range due to the 278 limitations of our data: 30–325 days. With this ad- 279 ditional constraint, we selected 52 candidate Blazhko 280 stars. Fig. 4 shows an example where two very promi- 281 nent peaks were identified in the LINEAR periodogram.

### 3.2.1. Visual Confirmation

The sample pre-selected for visual analysis includes 284 531 RR Lyrae stars ( $479 + 52$ ), or 18.1% of the starting 285 LINEAR-ZTF sample. Visual analysis included the fol- 286 lowing standard steps (e.g., Jurcsik et al. 2009; Prudil 287 & Skarka 2017):

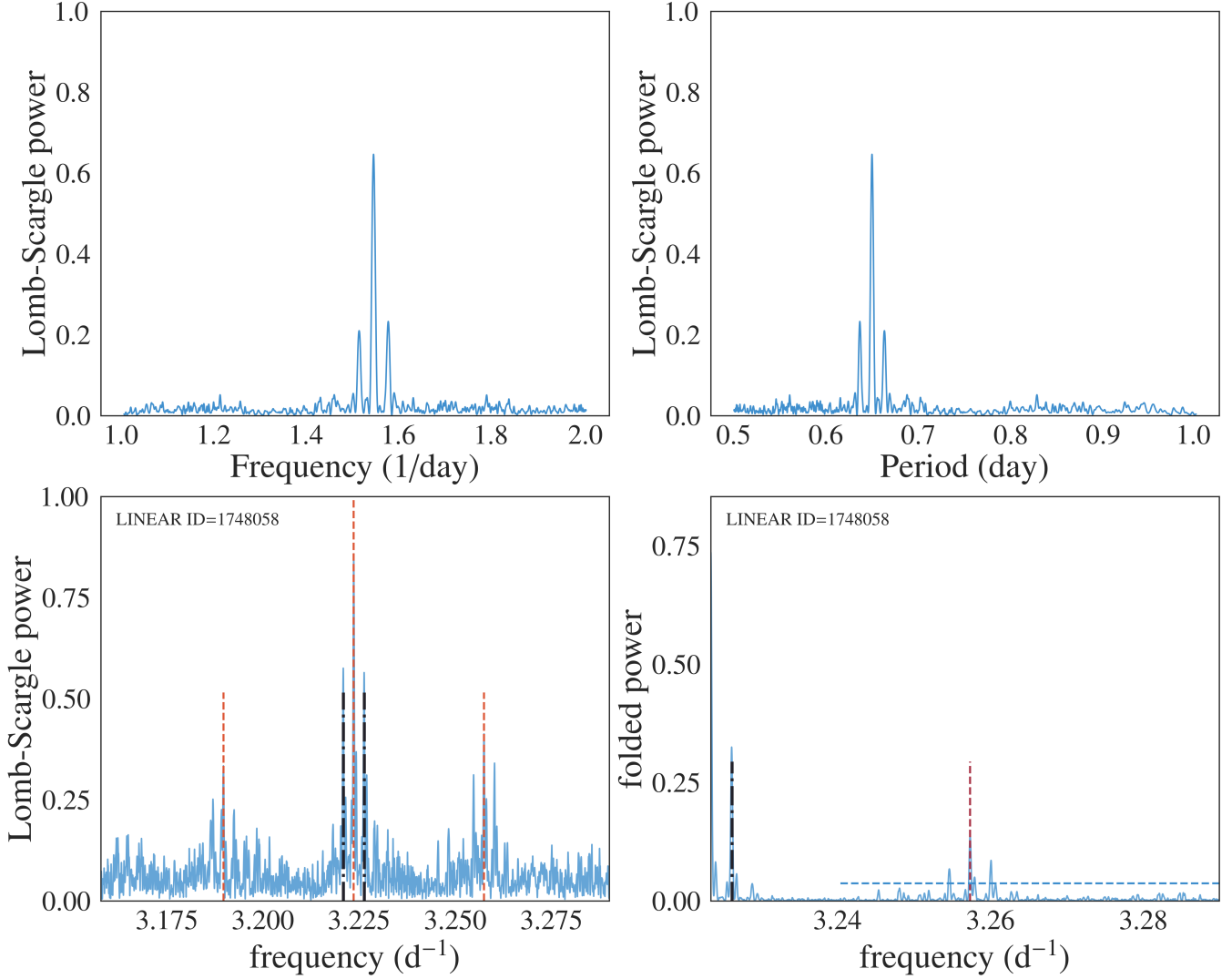


**Figure 4.** The top two panels show a simulated periodogram for a sum of two *sine* functions with similar frequencies  $f_1$  and  $f_2$  – the central peak corresponds to their mean (see eqs. 3 and 4). The bottom left panel shows a periodogram for an observed LINEAR light curve for  $ID = 1748058$ , and the bottom right panel shows its folded version (around the main frequency  $f_o = 3.223 \text{ d}^{-1}$ ). In the bottom left panel, the three vertical dashed lines show the three frequencies identified by the algorithm described in text, and the two dot-dashed lines mark yearly aliases around the main frequency  $f_o$ , at frequencies  $f_o \pm 0.0274 \text{ d}^{-1}$ . The two vertical lines in the bottom right panel have the same meaning, and the horizontal dashed line shows the noise level multiplied by 5.

- 289 1. The shape of the phased light curves and scatter of  
290 data points around the best-fit model were exam-  
291 ined for signatures of anomalous behavior indica-  
292 tive of the Blazhko effect. Fig. 6 shows an exam-  
293 ple of such behavior where the ZTF data and fit show  
294 multiple coherent data point sequences offset from  
295 the best-fit mean model.
- 296 2. Full light curves were inspected for their repeata-  
297 bility between observing seasons (Fig. 7). This  
298 step was sensitive to amplitude modulations with  
299 periods of the order a year or longer.
- 300 3. The phased light curves normalized to unit am-  
301 plitude were inspected for their repeatability be-  
302 tween observing seasons. This step was sensitive  
303 to phase modulations of a few percent or larger on  
304 time scales of the order a year or longer. Fig. 8  
305 shows an example of a Blazhko star where season-  
306 to-season phase and amplitude modulations are  
307 seen in both the LINEAR data and (especially)  
308 the ZTF data. Another example is shown in Fig. 9  
309 where only phase modulation is visible, without  
310 any discernible amplitude modulation.

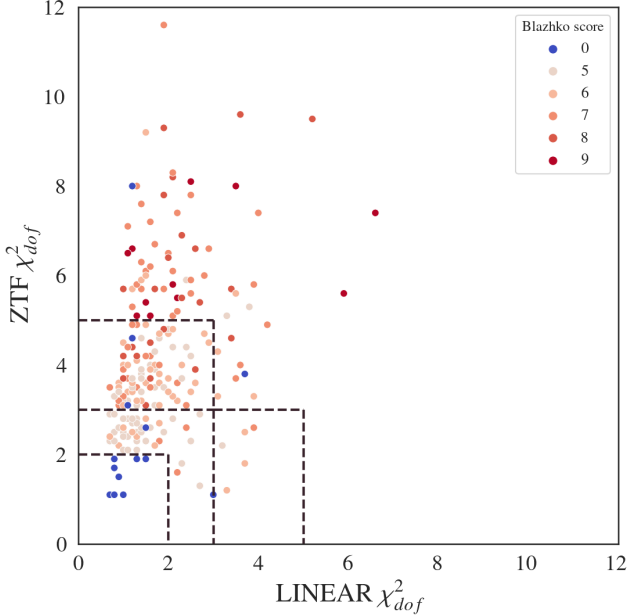


**Figure 5.** Analogous to figure 2, except that here only 228 visually verified Blazhko stars are shown.

After visually analyzing the starting sample of 531 Blazhko candidates, we visually confirmed expected Blazhko behavior for 228 stars (214 out of 479 and 14 out of 52). LINEAR IDs and other characteristics for confirmed Blazhko stars are listed in Table 1 (Appendix A). Statistical properties of the selected sample of Blazhko stars are discussed in detail in the next section.

#### 4. RESULTS

Starting with a sample of 2857 field RR Lyrae stars with both LINEAR and ZTF data, we constructed a subsample of 1996 with light curves of sufficient quality and selected and verified 228 stars that exhibit convincing Blazhko effect. In this section we compare various statistical properties of selected Blazhko stars to those of the starting sample.

##### 4.1. The Blazhko Incidence Rate

The implied incidence rate for the Blazhko effect is  $11.4 \pm 0.8\%$ . Due to selection effects and unknown completeness, this rate should be considered as a lower limit. When ab and c types are considered separately, the rate is slightly higher for the former than for the latter:  $12.1 \pm 0.9\%$  vs.  $9.2 \pm 1.3\%$ . The difference of  $2.9\%$  has low statistical significance ( $< 2\sigma$ ).

##### 4.2. Period, Amplitude and Magnitude Distributions

Marginal distributions of period, amplitude and apparent magnitude for the starting sample and Blazhko stars are compared in Fig. 10. Encouragingly, their magnitude distributions are statistically indistinguishable which indicates that the completeness is not a strong

function of the photometric signal-to-noise ratio. This result is probably due to the fact that the sample is defined by the depth of LINEAR survey, while ZTF survey is deeper than this limit and its photometric quality is approximately constant across the probed magnitude range.

The suspected differences in amplitude and period distributions are further explored in Fig. 11. It is already discernible by eye that the period distribution for Blazhko stars of ab type is shifted to smaller values than for the starting sample. We have found that the median period for ab type Blazhko stars is about 5% shorter than for the starting RR Lyrae sample. This difference is significant at the  $7.1\sigma$  level. At the same time, the difference in median amplitudes for ab type stars corresponds to only  $0.6\sigma$  deviation. No statistically significant differences are found in period and amplitude distributions for c type stars.

If modulation amplitudes are correlated with periods such that larger modulation amplitudes occur in shorter period RRab stars, and if our selection efficiency is lower for smaller modulation amplitudes, then the detected period shift for ab type Blazhko stars might be at least partially due to combination of these two effects. This possibility does not appear likely. First, as we discussed in preceeding section, our sample is defined by the depth of LINEAR survey, while ZTF survey is significantly deeper than this limit and its photometric quality is approximately constant across the probed magnitude range. Since it is sufficient for a star to display the Blazhko effect only in ZTF to be included in the sample, we do not expect strong selection effects (except for the LINEAR magnitude cutoff of course). Furthermore, Skarka et al. (2020) searched for period - modulation amplitude correlation using a large sample of stars with OGLE measurements and did not find any.

##### 4.3. Long-term behavior of Blazhko Stars

During visual analysis, we noticed that some Blazhko stars exhibit convincing Blazhko effect either in LINEAR or in ZTF data, but not in both surveys. Fig. 12 shows an example where amplitude modulation is clearly seen in LINEAR light curves, while not discernible in ZTF light curves. There are also examples of stars where Blazhko effect is evident in ZTF but not in LINEAR data (e.g., LINEARid = 19466437, 14155360). This finding strongly suggests that Blazhko effect can appear and disappear on time scales shorter than about a decade.

#### 5. DISCUSSION AND CONCLUSIONS

We found excellent agreement between the best-fit periods for RR Lyrae stars estimated separately from LINEAR and ZTF light curves. Only one star in our sample (CT CrB, LINEARid=17919686), was previously reported as a Blazhko star (Skarka 2013). The sample of 228 stars presented here increases the number of field

## STAR 160 from 239

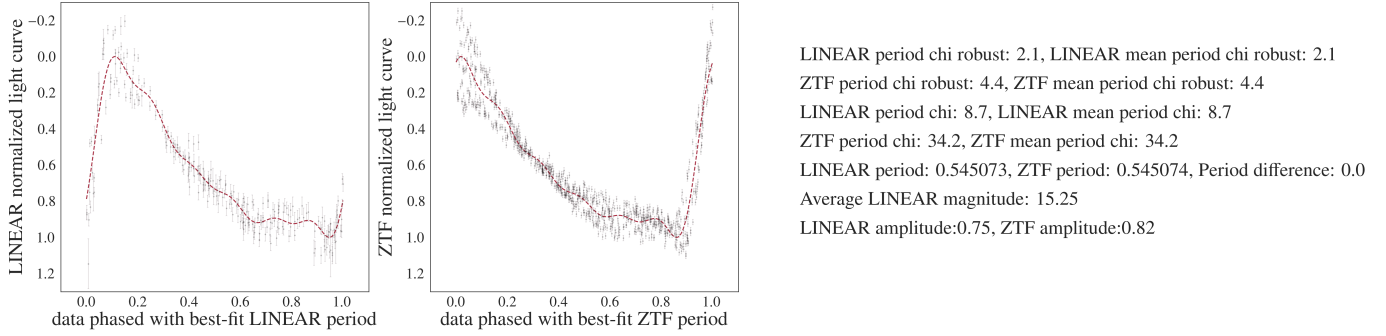


**Figure 6.** An illustration of visual analysis of phased light curves for the selected Blazhko candidates. The left panel shows LINEAR data and the right panel shows ZTF data (symbols with “error bars”) for star with LINEARid = 10030349. The dashed lines are best-fit models. The numbers listed on the right side were added to aid visual analysis. Note multiple coherent data point sequences offset from the best-fit mean model in the right panel.

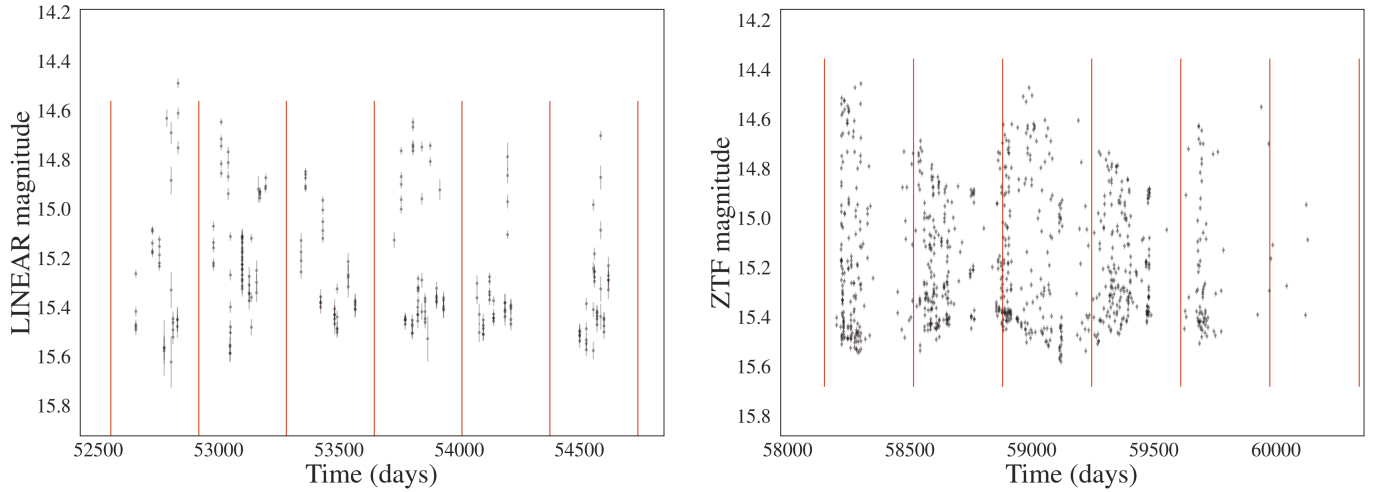


**Figure 7.** An illustration of visual analysis of full light curves for the selected Blazhko candidates with emphasis on their repeatability between observing seasons, marked with vertical lines (left: LINEAR data; right: ZTF data). Data shown are for star with LINEARid = 10030349. Note strong amplitude modulation between observing seasons.

RR Lyrae stars displaying the Blazhko effect by more than 50% and places a lower limit of  $(11.4 \pm 0.8)\%$  for their incidence rate. The reported incidence rates for the Blazhko effect range from 5% (Szczygieł & Fabrycky 2007) to 60% (Szabó et al. 2014). Differences in reported incidence rates can occur due to varying data precision, the temporal baseline length, and differences in visual or algorithmic analysis. For a relatively small sample of 151 stars with Kepler data, a claim has been made that essentially every RR Lyrae star exhibits modulated light curve (Kovacs 2018). The difference in Blazhko incidence rates for the two most extensive samples, obtained by the OGLE-III survey for the Large Magellanic Cloud (LMC, 20% out of 17,693 stars; Soszyński et al. 2009) and the Galactic bulge (30% out of 11,756 stars; Soszyński et al. 2011) indicates a possible variation of the Blazhko incidence rate with underlying stellar population properties.

We find that ab type RR Lyrae which show the Blazhko effect have about 5% (0.030 day) shorter periods than starting sample. While not large, the statistical significance of this difference is  $7.1\sigma$ . At a similar uncertainty level ( $\sim 1\%$ ), we don’t detect period difference for c type stars, and don’t detect any difference in amplitude distributions. We also find that for some stars the Blazhko effect is discernible in only one dataset. This finding strongly suggests that Blazhko effect can appear and disappear on time scales shorter than about a decade, in agreement with literature (Jurcsik et al. 2009; Poretti et al. 2010; Benkő et al. 2014). The LINEAR and ZTF datasets analyzed in this work were sufficiently large that we had to rely on algorithmic pruning of the initial sample. The sample size problem will be even larger for surveys such as the Legacy Survey of Space and Time (LSST; Ivezić et al. 2019). LSST will be an excellent survey for studying Blazhko effect

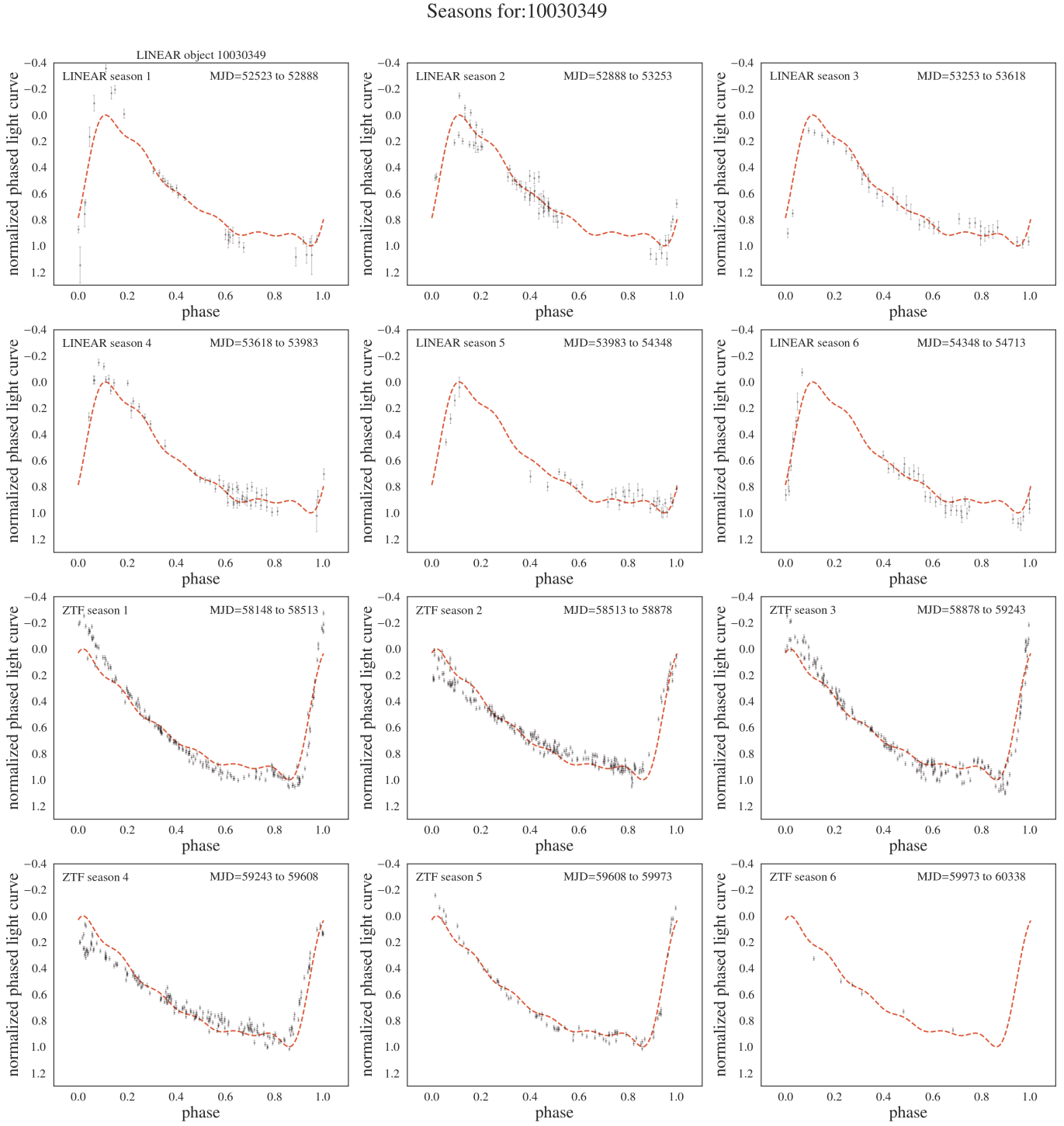


**Figure 8.** The phased light curves normalized to unit amplitude of the overall best-fit model are shown for single observing seasons and compared to the mean best-fit models (top six panels: LINEAR data; bottom six panels: ZTF data). Data shown are for star with LINEARid = 10030349. Season-to-season phase and amplitude modulations are seen in both the LINEAR and the ZTF data.

<sup>431</sup> (Hernitschek & Stassun 2022) because it will have both  
<sup>432</sup> a long temporal baseline (10 years) and a large number  
<sup>433</sup> of observations per object (nominally 825; LSST Sci-  
<sup>434</sup> ence Requirements Document<sup>4</sup>). We anticipate a higher  
<sup>435</sup> fraction of discovered Blazhko stars with LSST than re-  
<sup>436</sup> ported here due to better sampling and superior photo-  
<sup>437</sup> metric quality, since the incidence rate of the Blazhko  
<sup>438</sup> effect increases with sensitivity to small-amplitude mod-  
<sup>439</sup> ulation, and thus with photometric data quality (Jurecsik  
<sup>440</sup> et al. 2009).

<sup>441</sup> The size and quality of LSST sample will motivate  
<sup>442</sup> further developments of the selection algorithms. One  
<sup>443</sup> obvious improvement will be inspection of neighboring  
<sup>444</sup> objects to confirm photometric quality, as well as inspec-  
<sup>445</sup> tion of images to test implication of an isolated point  
<sup>446</sup> source (e.g., blended object photometry can be affected  
<sup>447</sup> by variable seeing beyond aperture correction valid for  
<sup>448</sup> isolated point sources). Another improvement is for-  
<sup>449</sup> ward modeling of the Blazhko modulation, rather than  
<sup>450</sup> searching for  $\chi^2$  outliers (Benkő et al. 2011; Guggen-  
<sup>451</sup> berger et al. 2012). For example, Skarka et al. (2020)  
<sup>452</sup> classified Blazhko stars in 6 classes using the morphol-  
<sup>453</sup> ogy of their amplitude modulation (the most dominant  
<sup>454</sup> class includes 90% of the sample). They also found bi-  
<sup>455</sup> modal distribution of Blazko periods, with two compo-  
<sup>456</sup> nents centered on 48 d and 186 d. These results give  
<sup>457</sup> hope that forward modeling of the Blazhko effect will  
<sup>458</sup> improve the selection of such stars.

<sup>459</sup> We thank Mathew Graham for providing *ztfquery* code  
<sup>460</sup> example to us, and Robert Szabó for expert comments  
<sup>461</sup> that improved presentation.

<sup>462</sup> Ž.I. acknowledges funding by the Fulbright Founda-  
<sup>463</sup> tion and thanks the Ruđer Bošković Institute (Zagreb,  
<sup>464</sup> Croatia) for hospitality.

<sup>465</sup> Based on observations obtained with the Samuel  
<sup>466</sup> Oschin Telescope 48-inch and the 60-inch Telescope at  
<sup>467</sup> the Palomar Observatory as part of the Zwicky Tran-  
<sup>468</sup> sient Facility project. ZTF is supported by the Na-  
<sup>469</sup> tional Science Foundation under Grants No. AST-  
<sup>470</sup> 1440341 and AST-2034437 and a collaboration includ-  
<sup>471</sup> ing current partners Caltech, IPAC, the Weizmann In-  
<sup>472</sup> stitute of Science, the Oskar Klein Center at Stock-  
<sup>473</sup> holm University, the University of Maryland, Deutsches  
<sup>474</sup> Elektronen-Synchrotron and Humboldt University, the  
<sup>475</sup> TANGO Consortium of Taiwan, the University of Wis-  
<sup>476</sup>consin at Milwaukee, Trinity College Dublin, Lawrence  
<sup>477</sup> Livermore National Laboratories, IN2P3, University of  
<sup>478</sup> Warwick, Ruhr University Bochum, Northwestern Uni-  
<sup>479</sup> versity and former partners the University of Wash-  
<sup>480</sup> ington, Los Alamos National Laboratories, and Lawrence  
<sup>481</sup> Berkeley National Laboratories. Operations are con-  
<sup>482</sup> ducted by COO, IPAC, and UW.

<sup>483</sup> The LINEAR program is funded by the National Aero-  
<sup>484</sup> nautics and Space Administration at MIT Lincoln Lab-  
<sup>485</sup> oratory under Air Force Contract FA8721-05-C-0002.  
<sup>486</sup> Opinions, interpretations, conclusions and recommen-  
<sup>487</sup> dations are those of the authors and are not necessarily  
<sup>488</sup> endorsed by the United States Government.

<sup>489</sup> *Software:* Astropy (Astropy Collaboration et al.  
<sup>490</sup> 2018, 2022), Matplotlib (Hunter 2007), SciPy (Virtanen  
<sup>491</sup> et al. 2020), astroML (VanderPlas et al. 2012)

## Seasons for:16300450

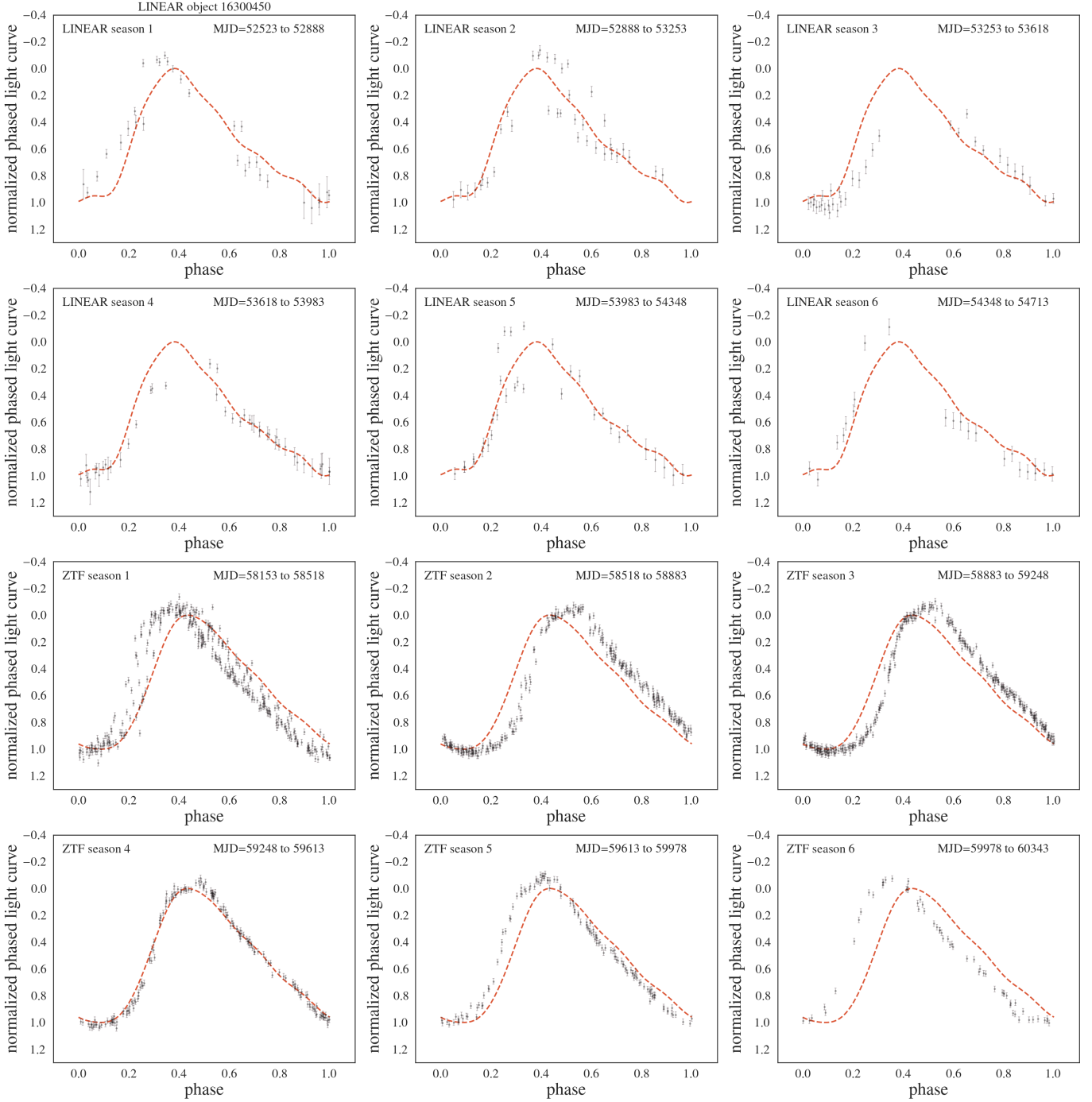


**Figure 9.** Analogous to Fig. 8, except that star with LINEARid = 16300450 is shown. Unlike example shown in Fig. 8, only phase modulation is visible here, without any amplitude modulation, in both LINEAR and ZTF light curves.

<sup>4</sup> Available as ls.st/srd

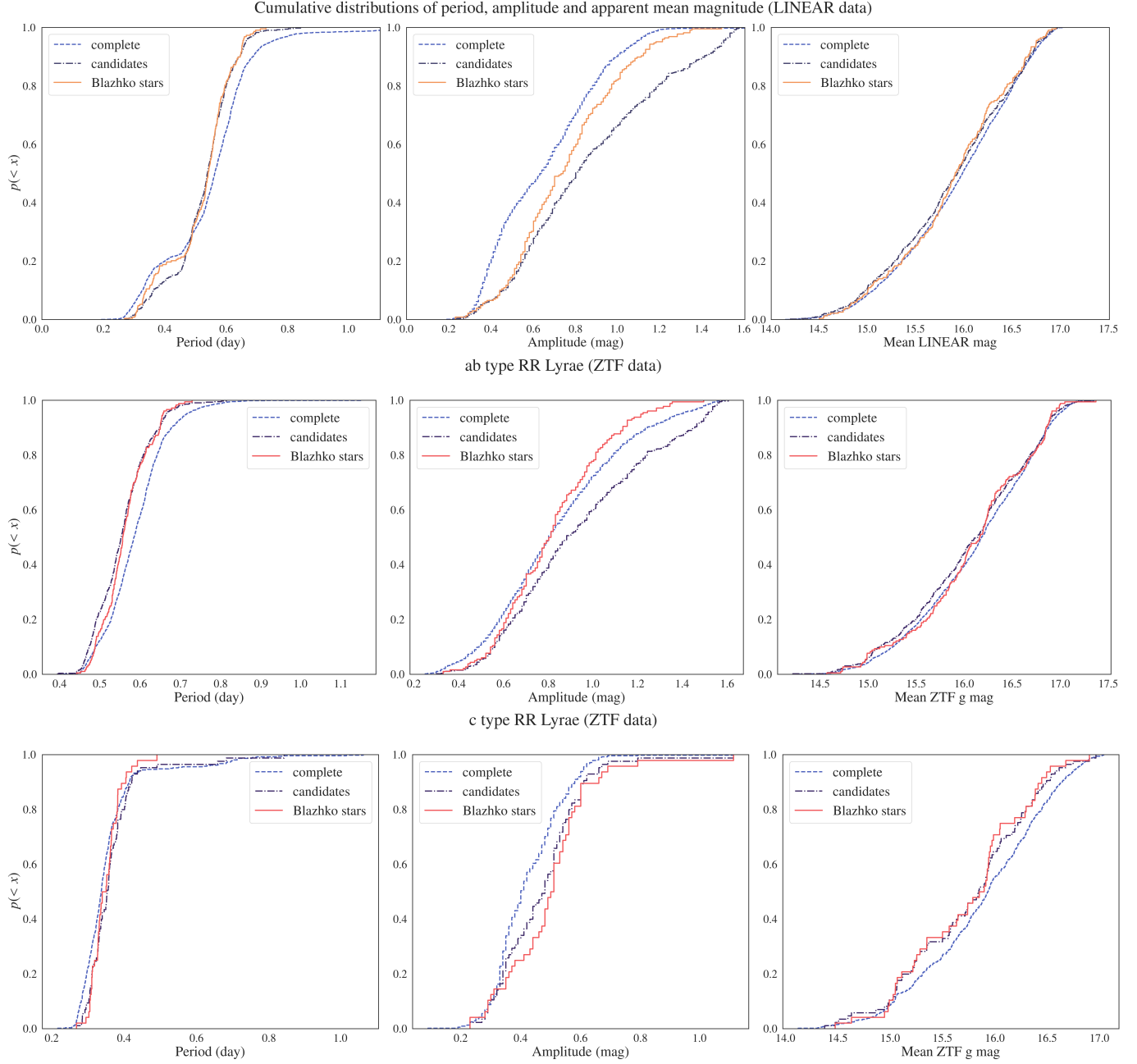


**Figure 10.** A comparison of cumulative distributions of period (left), amplitude (middle) and apparent magnitude for starting sample, selected Blazhko candidates and visually verified Blazhko stars. The top row is based on LINEAR data and both ab type and c type stars. The middle and bottom rows are based on ZTF data, and show separately data for ab type and c type stars, respectively. The differences in period and amplitude distributions are further examined in figure 11.

Table 1: The first 10 confirmed Blazhko stars with their LINEAR IDs in the first column and then, for both LINEAR and ZTF, their computed light curve periods (day), the number of data points per light curve, robust and ordinary  $\chi^2$  values, and light curve amplitudes, followed by amplitude difference between LINEAR and ZTF, the strength and period of Blazhko peaks in their periodograms, light curve type (1: ab, 2: c), detection significance flag for the periodograms (Z, L or “-” for no detection; the strength and period of Blazhko peaks are not reliable when “-”) and the selection score (see Sections 3.1 and 3.2 for details). The full table is available in online edition.

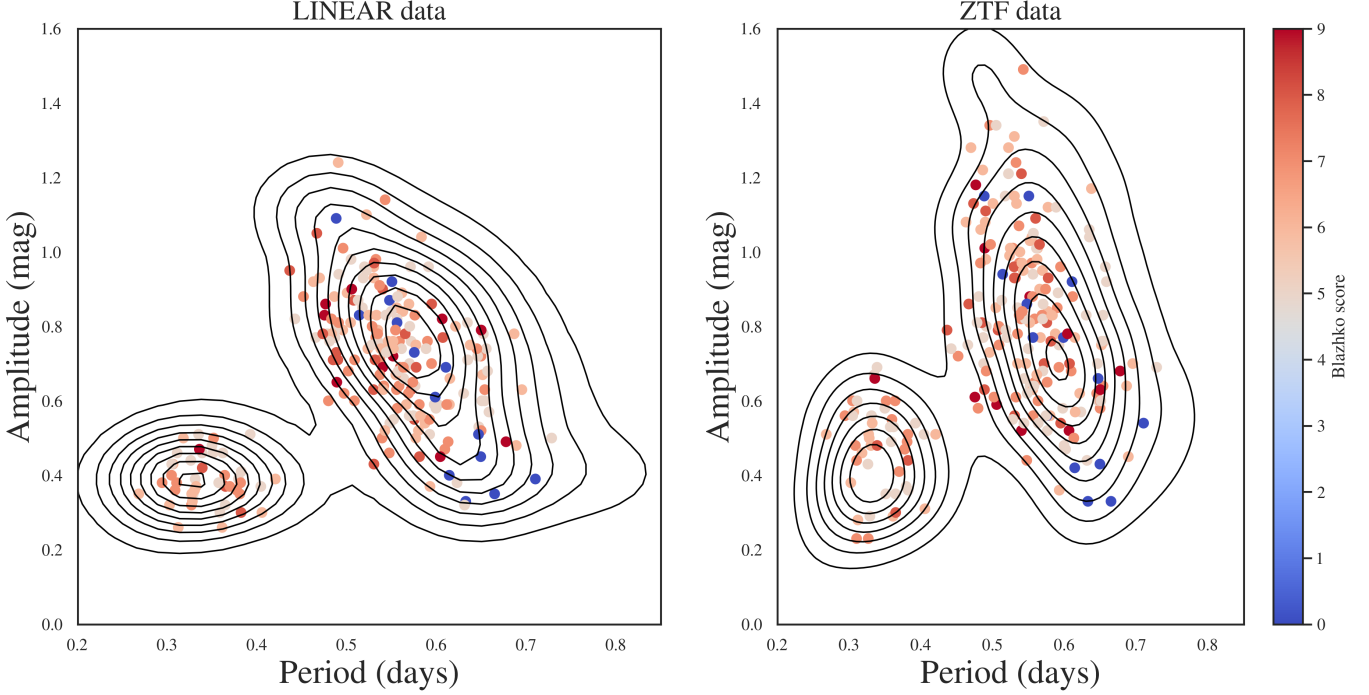


**Figure 11.** Comparison of amplitude–period distributions (the Bailey diagram) for the starting sample of 1,996 RR Lyrae stars (contours) and 228 selected candidate Blazhko stars (symbols). The clump in the lower left corresponds to c type RR Lyrae and the other one to ab type. Note that the period distribution for ab type Blazhko stars is shifted left (by about 0.03 day, or 5%).

499

LID	P <sub>L</sub>	P <sub>Z</sub>	N <sub>L</sub>	N <sub>Z</sub>	χ <sub>L,r</sub> <sup>2</sup>	χ <sub>Z,r</sub> <sup>2</sup>	χ <sub>L</sub> <sup>2</sup>	χ <sub>Z</sub> <sup>2</sup>	A <sub>L</sub>	A <sub>Z</sub>	δA	B <sub>pL</sub>	B <sub>pZ</sub>	B <sub>pL</sub>	B <sub>pZ</sub>	t	f	B <sub>s</sub>	B <sub>f</sub>
158779	0.609207	0.609189	293	616	1.6	3.9	3.7	34.2	0.47	0.68	0.21	1.6443	1.6444	352.7337	350.2	1	-	7	1
263541	0.558218	0.558221	270	503	2.9	6.6	15.8	110.4	0.64	0.82	0.18	1.8621	1.8025	14.1513	89.9	1	-	7	1
393084	0.530027	0.530033	493	372	1.1	3.2	1.6	19.2	0.96	1.31	0.35	1.9447	1.8896	17.2369	347.2	1	-	6	1
810169	0.465185	0.465212	289	743	2.1	2.8	6.0	15.1	0.77	0.75	0.02	2.2232	2.2230	13.6017	13.6	1	-	5	1
924301	0.507503	0.507440	418	189	1.9	9.3	13.8	162.9	0.87	0.79	0.08	2.0043	1.9763	29.5072	178.4	1	-	8	1
970326	0.592233	0.592231	275	552	1.1	2.1	1.9	7.7	0.51	0.75	0.24	1.7563	1.6992	14.7656	93.2	1	-	5	1
999528	0.658401	0.658407	564	213	1.2	2.7	1.8	21.7	0.57	0.92	0.35	1.5527	1.5510	29.5247	31.0	1	-	5	1
1005497	0.653607	0.653605	607	192	1.1	2.1	2.1	12.4	0.60	0.83	0.23	1.5639	1.5481	29.4638	55.1	1	-	5	1
1092244	0.649496	0.649558	590	326	1.2	3.6	2.3	32.1	0.72	0.58	0.14	1.5735	1.5640	29.5421	40.8	1	-	7	1
1240665	0.632528	0.632522	468	311	3.0	1.1	25.2	1.6	0.33	0.33	0.00	1.6149	1.5865	29.4942	182.3	1	Z	0	2

500

## REFERENCES

- 501 Alcock, C., Alves, D. R., Becker, A., et al. 2003, ApJ, 598,  
502 597, doi: [10.1086/378689](https://doi.org/10.1086/378689)
- 503 Astropy Collaboration, Price-Whelan, A. M., Sipőcz, B. M.,  
504 et al. 2018, AJ, 156, 123, doi: [10.3847/1538-3881/aabc4f](https://doi.org/10.3847/1538-3881/aabc4f)
- 505 Astropy Collaboration, Price-Whelan, A. M., Lim, P. L.,  
506 et al. 2022, ApJ, 935, 167, doi: [10.3847/1538-4357/ac7c74](https://doi.org/10.3847/1538-4357/ac7c74)
- 507 Bellm, E. C., Kulkarni, S. R., Graham, M. J., et al. 2019,  
508 PASP, 131, 018002, doi: [10.1088/1538-3873/aaecbe](https://doi.org/10.1088/1538-3873/aaecbe)
- 509 Benkő, J. M., Plachy, E., Szabó, R., Molnár, L., & Kolláth,  
510 Z. 2014, ApJS, 213, 31, doi: [10.1088/0067-0049/213/2/31](https://doi.org/10.1088/0067-0049/213/2/31)
- 511 Benkő, J. M., Szabó, R., & Paparó, M. 2011, MNRAS, 417,  
512 974, doi: [10.1111/j.1365-2966.2011.19313.x](https://doi.org/10.1111/j.1365-2966.2011.19313.x)
- 513 Benkő, J. M., Kolenberg, K., Szabó, R., et al. 2010,  
514 MNRAS, 409, 1585,  
515 doi: [10.1111/j.1365-2966.2010.17401.x](https://doi.org/10.1111/j.1365-2966.2010.17401.x)
- 516 Blažko, S. 1907, Astronomische Nachrichten, 175, 325,  
517 doi: [10.1002/asna.19071752002](https://doi.org/10.1002/asna.19071752002)
- 518 Catelan, M. 2009, Ap&SS, 320, 261,  
519 doi: [10.1007/s10509-009-9987-8](https://doi.org/10.1007/s10509-009-9987-8)
- 520 Guggenberger, E., Kolenberg, K., Nemec, J. M., et al. 2012,  
521 MNRAS, 424, 649, doi: [10.1111/j.1365-2966.2012.21244.x](https://doi.org/10.1111/j.1365-2966.2012.21244.x)

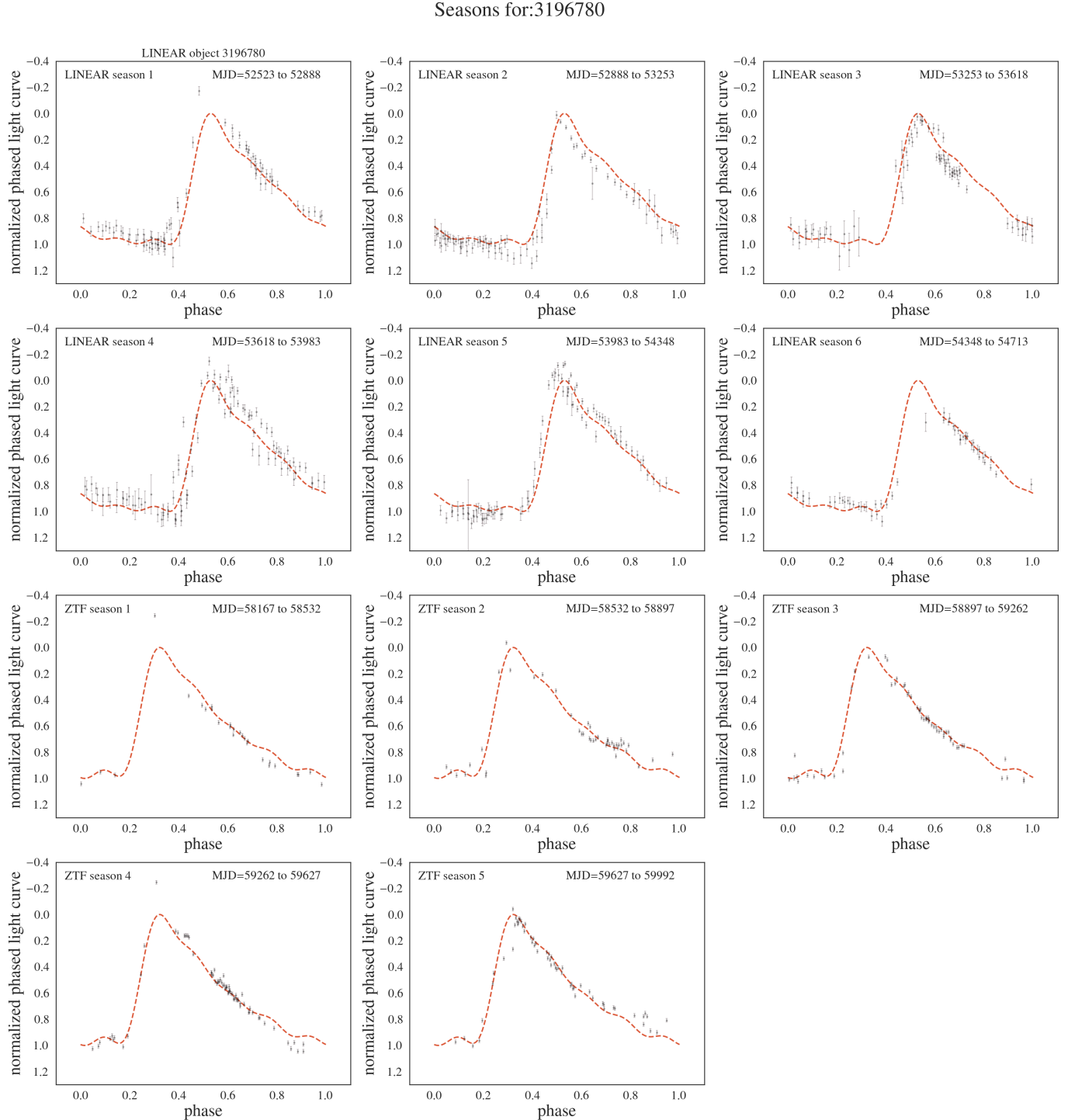


**Figure 12.** Analogous to Fig. 8, except that star with LINEARid = 3196780 is shown. Amplitude modulation is clearly seen in LINEAR light curves (top two rows), while not discernible in ZTF light curves (bottom two rows). Additional stars with similar behavior include LINEARid = 2889542, 7723614, 8342007. This behavior strongly suggests that Blazhko effect can appear and disappear on time scales shorter than about a decade.

- <sup>522</sup> Hernitschek, N., & Stassun, K. G. 2022, ApJS, 258, 4,  
<sup>523</sup> doi: [10.3847/1538-4365/ac3baf](https://doi.org/10.3847/1538-4365/ac3baf)
- <sup>524</sup> Hunter, J. D. 2007, Computing in Science & Engineering, 9,  
<sup>525</sup> 90, doi: [10.1109/MCSE.2007.55](https://doi.org/10.1109/MCSE.2007.55)
- <sup>526</sup> Ivezić, Ž., Kahn, S. M., Tyson, J. A., et al. 2019, ApJ, 873,  
<sup>527</sup> 111, doi: [10.3847/1538-4357/ab042c](https://doi.org/10.3847/1538-4357/ab042c)
- <sup>528</sup> Jurcsik, J., Sódor, Á., Szeidl, B., et al. 2009, MNRAS, 400,  
<sup>529</sup> 1006, doi: [10.1111/j.1365-2966.2009.15515.x](https://doi.org/10.1111/j.1365-2966.2009.15515.x)
- <sup>530</sup> Kolenberg, K. 2008, in Journal of Physics Conference  
<sup>531</sup> Series, Vol. 118, Journal of Physics Conference Series  
<sup>532</sup> (IOP), 012060, doi: [10.1088/1742-6596/118/1/012060](https://doi.org/10.1088/1742-6596/118/1/012060)
- <sup>533</sup> Kovács, G. 2009, in American Institute of Physics  
<sup>534</sup> Conference Series, Vol. 1170, Stellar Pulsation:  
<sup>535</sup> Challenges for Theory and Observation, ed. J. A. Guzik  
<sup>536</sup> & P. A. Bradley, 261–272, doi: [10.1063/1.3246458](https://doi.org/10.1063/1.3246458)
- <sup>537</sup> Kovacs, G. 2016, Communications of the Konkoly  
<sup>538</sup> Observatory Hungary, 105, 61,  
<sup>539</sup> doi: [10.48550/arXiv.1512.05722](https://doi.org/10.48550/arXiv.1512.05722)
- <sup>540</sup> —. 2018, A&A, 614, L4, doi: [10.1051/0004-6361/201833181](https://doi.org/10.1051/0004-6361/201833181)
- <sup>541</sup> Mizerski, T. 2003, AcA, 53, 307,  
<sup>542</sup> doi: [10.48550/arXiv.astro-ph/0401612](https://doi.org/10.48550/arXiv.astro-ph/0401612)
- <sup>543</sup> Palaversa, L., Ivezić, Ž., Eyer, L., et al. 2013, AJ, 146, 101,  
<sup>544</sup> doi: [10.1088/0004-6256/146/4/101](https://doi.org/10.1088/0004-6256/146/4/101)
- <sup>545</sup> Poretti, E., Paparó, M., Deleuil, M., et al. 2010, A&A, 520,  
<sup>546</sup> A108, doi: [10.1051/0004-6361/201014941](https://doi.org/10.1051/0004-6361/201014941)
- <sup>547</sup> Prudil, Z., & Skarka, M. 2017, MNRAS, 466, 2602,  
<sup>548</sup> doi: [10.1093/mnras/stw3231](https://doi.org/10.1093/mnras/stw3231)
- <sup>549</sup> Sesar, B., Stuart, J. S., Ivezić, Ž., et al. 2011, AJ, 142, 190,  
<sup>550</sup> doi: [10.1088/0004-6256/142/6/190](https://doi.org/10.1088/0004-6256/142/6/190)
- <sup>551</sup> Sesar, B., Ivezić, Ž., Grammer, S. H., et al. 2010, ApJ, 708,  
<sup>552</sup> 717, doi: [10.1088/0004-637X/708/1/717](https://doi.org/10.1088/0004-637X/708/1/717)
- <sup>553</sup> Sesar, B., Ivezić, Ž., Stuart, J. S., et al. 2013, AJ, 146, 21,  
<sup>554</sup> doi: [10.1088/0004-6256/146/2/21](https://doi.org/10.1088/0004-6256/146/2/21)
- <sup>555</sup> Skarka, M. 2013, A&A, 549, A101,  
<sup>556</sup> doi: [10.1051/0004-6361/201220398](https://doi.org/10.1051/0004-6361/201220398)
- <sup>557</sup> Skarka, M., Prudil, Z., & Jurcsik, J. 2020, MNRAS, 494,  
<sup>558</sup> 1237, doi: [10.1093/mnras/staa673](https://doi.org/10.1093/mnras/staa673)
- <sup>559</sup> Smith, H. A. 1995, Cambridge Astrophysics Series, 27
- <sup>560</sup> Soszyński, I., Udalski, A., Szymański, M. K., et al. 2010,  
<sup>561</sup> AcA, 60, 165, doi: [10.48550/arXiv.1009.0528](https://doi.org/10.48550/arXiv.1009.0528)
- <sup>562</sup> —. 2009, AcA, 59, 1, doi: [10.48550/arXiv.0903.2482](https://doi.org/10.48550/arXiv.0903.2482)
- <sup>563</sup> Soszyński, I., Dziembowski, W. A., Udalski, A., et al. 2011,  
<sup>564</sup> AcA, 61, 1, doi: [10.48550/arXiv.1105.6126](https://doi.org/10.48550/arXiv.1105.6126)
- <sup>565</sup> Szabó, R. 2014, in IAU Symposium, Vol. 301, Precision  
<sup>566</sup> Asteroseismology, ed. J. A. Guzik, W. J. Chaplin,  
<sup>567</sup> G. Handler, & A. Pigulski, 241–248,  
<sup>568</sup> doi: [10.1017/S1743921313014397](https://doi.org/10.1017/S1743921313014397)
- <sup>569</sup> Szabó, R., Benkő, J. M., Paparó, M., et al. 2014, A&A,  
<sup>570</sup> 570, A100, doi: [10.1051/0004-6361/201424522](https://doi.org/10.1051/0004-6361/201424522)
- <sup>571</sup> Szczygieł, D. M., & Fabrycky, D. C. 2007, MNRAS, 377,  
<sup>572</sup> 1263, doi: [10.1111/j.1365-2966.2007.11678.x](https://doi.org/10.1111/j.1365-2966.2007.11678.x)
- <sup>573</sup> Vanderplas, J. 2015, gatspy: General tools for Astronomical  
<sup>574</sup> Time Series in Python, v0.1.1, Zenodo,  
<sup>575</sup> doi: [10.5281/zenodo.14833](https://doi.org/10.5281/zenodo.14833)
- <sup>576</sup> VanderPlas, J., Connolly, A. J., Ivezic, Z., & Gray, A.  
<sup>577</sup> 2012, in Proceedings of Conference on Intelligent Data  
<sup>578</sup> Understanding (CIDU, 47–54,  
<sup>579</sup> doi: [10.1109/CIDU.2012.6382200](https://doi.org/10.1109/CIDU.2012.6382200)
- <sup>580</sup> Virtanen, P., Gommers, R., Oliphant, T. E., et al. 2020,  
<sup>581</sup> Nature Methods, 17, 261, doi: [10.1038/s41592-019-0686-2](https://doi.org/10.1038/s41592-019-0686-2)